Electronic supplementary information

Cluster-luminescent polysiloxane nanomaterials: adjustable full-color ultralong room temperature phosphorescence and highly sensitive response to silver ions

Shuaiqi Wang[a], Xiaolang Wang[a], Shangwei Feng[a], Wei Lv[a], Meijuan Lin[a], Qidan Ling[a] and Zhenghuan Lin*[a,b]

[a] *Fujian Key Laboratory of Polymer Materials, College of Chemistry and Materials Science, Fujian Normal University, Fuzhou 350007, China.*
E-mail: zhlin@fjnu.edu.cn
[b] *Fujian Provincial Key Laboratory of Advanced Materials Oriented Chemical Engineering, Fuzhou, 350007, China*

EXPERIMENTAL SECTION

General methods

Steady-state photoluminescence spectra and quantum yield of the samples were obtained at the room temperature using an Edinburgh FS5 spectrofluorometer with a xenon arc lamp (Xe900) and an integrating sphere for absolute photoluminescence quantum yield determination. Time-resolved photoluminescence decay curves and delay spectra were obtained using a FLS920 fluorescence spectrometer equipped with a microsecond flash-lamp (μF900), and a nanosecond hydrogen flash-lamp (nF920). TGA data were obtained from Mettler's thermogravimeter. The heating rate is 10 ^{o}C/min, nitrogen is used to protect the test process. The crystalline structure of samples was confirmed by PXRD using a PANalytical X-ray diffractometer (X'Pert3 Powder) with Cu Kα radiation (λ = 1.54178 Å) with a step size of 5°/min. FT-IR using the KBr pellet was carried out on Thermo-Nocilet IS50. In-situ IR was obtained using the attenuated total reflectance (ATR) attachment of Thermo-Nocilet IS50. XPS was obtained by ESCALAB 250 X-ray photoelectron spectrometer. The HRSEM photos were obtained by Verios G4 UC ultrahigh resolution field emission scanning electron microscope and the particle size data were obtained from Nano Measurer. Solid-state NMR spectra were measured on a Bruker Ascend 400 FT-NMR spectrometer.

Materials

All chemicals were obtained from commercial suppliers and used directly in the experiments without further purification unless otherwise stated.

Synthesis of polysiloxanes

All polysiloxanes were synthesized in the same procedure: In a 20 mL of flask, 10 mmol of siloxane was added, followed by adding 1 ml of 0.1 mol/L HCl solution and 5 mL of deionized water. The mixture was stirred vigorously for 3 h at room temperature and aged at 90 ℃ for 24 h. Then, it was rinsed with deionized water and dried in a vacuum oven at 80 ℃ for 24h to obtain the corresponding polysiloxanes in a yield more than 95%.

Synthesis of nanocomposites based on polysiloxane

The synthetic procedure of nanocomposites is similar as that of polysiloxanes. Taking PAS-MA as an example, the synthesis steps are as follows: Firstly, maleic anhydride

(0.98 g, 10 mmol) was dissolved in 2 mL of ethanol. Then, aminopropyl triethoxysilane (2.35 ml, 10 mmol) was added to a 20 mL flask followed by 1 ml of 0.1 mol/L HCl solution and 5 mL of deionized water. After stirring vigorously for 3 h at room temperature, the above ethanol solution of MA was added into the mixture. It was aged at 90 ℃ for 24 hours, rinsed with deionized water and dried in a vacuum oven at 80 ℃ for 24 h to obtain the nanocomposite PAS-MA in a yield more than 95%.

Ion Detection

The metal ionic salts were dissolved into water to form different concentrations of aqueous solutions, and the PAS powder was immersed in the aqueous solutions for 1 minute. Then the powder was taken out and heated at 100 ℃ for one minute for photoluminescence and delayed spectroscopy measurements.

Recyclability

PAS was soaked in Ag^+ aqueous solution with a concentration of 2 mM for 1 minute, and then the PAS powders were filtered and washed by 30 ml of deionized water with a centrifuge. After centrifugation for 5 min, the upper transparent layer was poured off. The powders were washed for three times before being heated at 100°C for 1 min for delayed spectroscopy measurements.

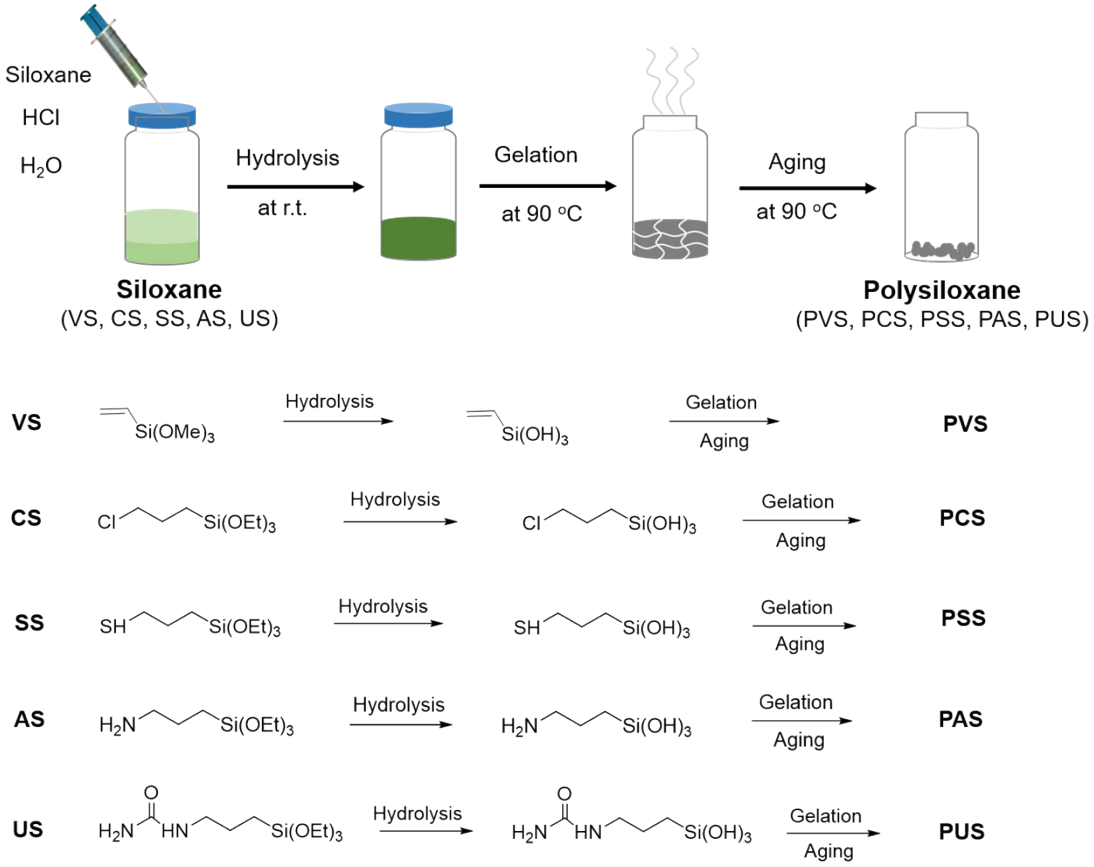

Scheme S1 Synthesis process of polysiloxanes.

Table S1 Comparison of limit of detection of different reported sensors for Ag^{+} ion.

Sensor	LOD (nM)	Ref.
Dansyl-Glu-Cys-Glu-Glu-Trp-NH2	80	1
ssDNA/nano-graphite	0.3	2
OS-g-C3N4-dots	2	3
AuNPs-Tris	410	4
Single-cytosine	0.02	5
Graphene quantum dots and o-phenylenediamine	250	6
Glutathione-mediated MnO2 nanosheets	4.23	7
BIB	45.9	8
BSA–Au nanoclusters	226	9
Anthraquinone–imidazole-based	66	10
Triazole-imidazole	50	11
Gold nanoclusters	260	12
PAS	0.027	This work

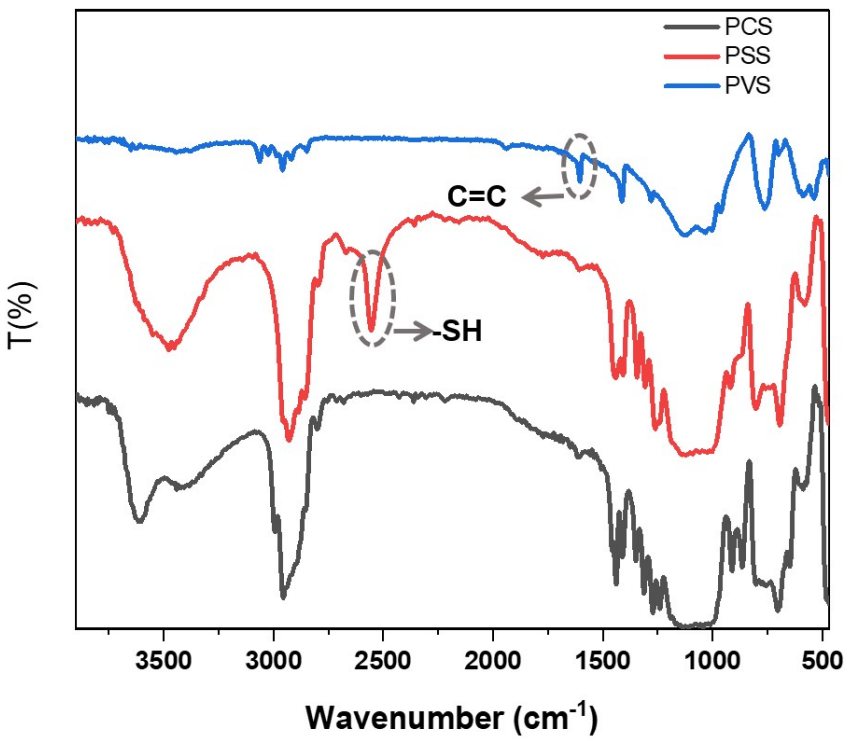

Fig. S1 FT-IR spectra of PCS, PSS and PVS.

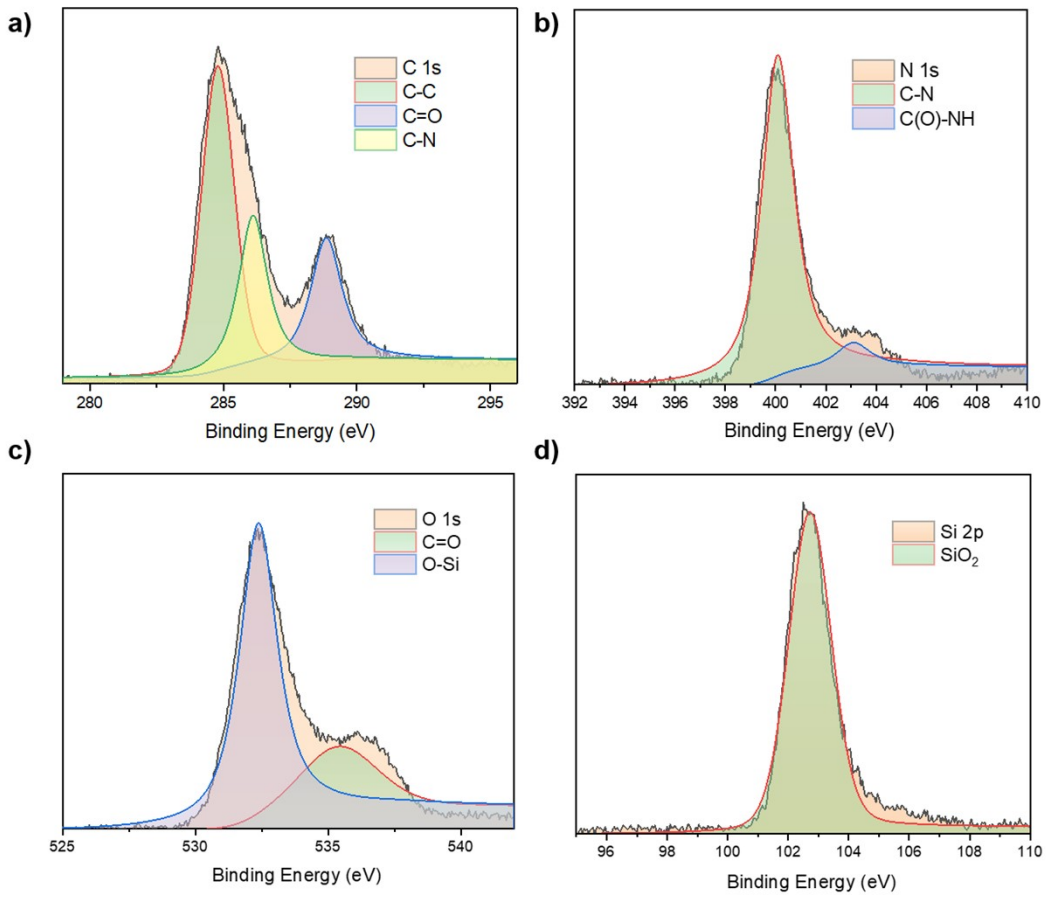

Fig. S2 XPS spectra of PUS.

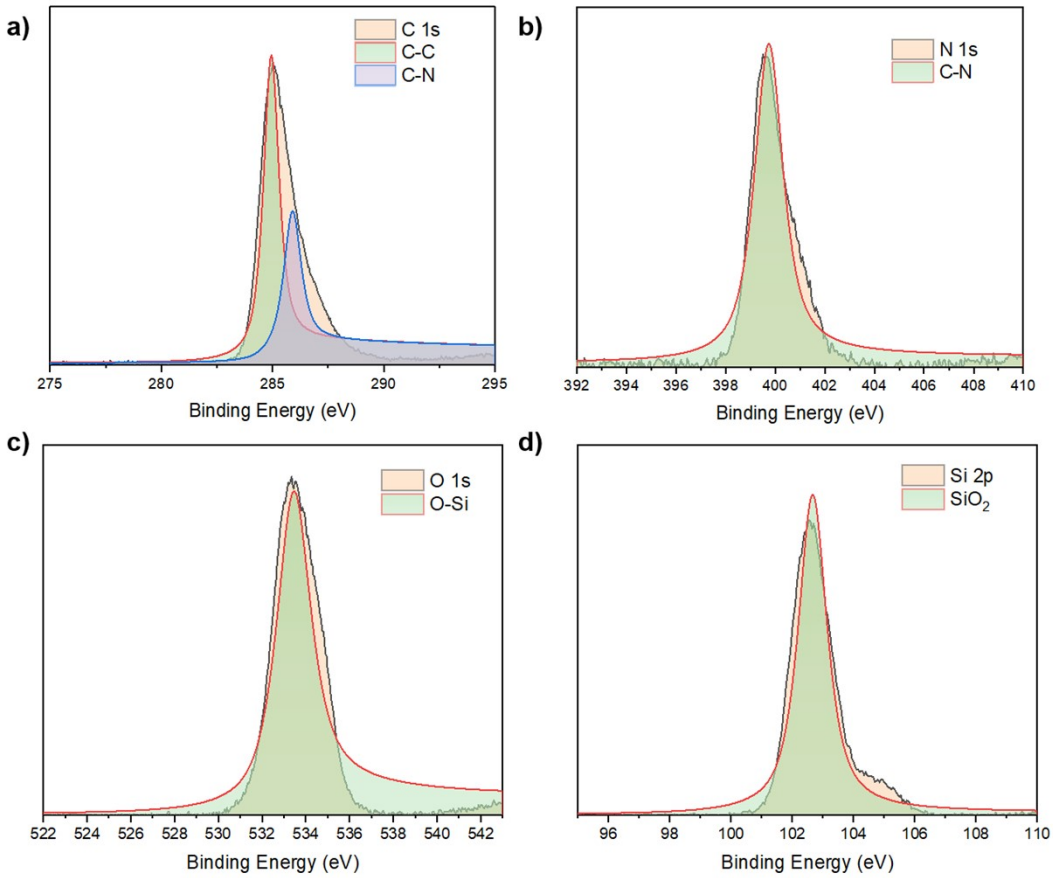

Fig. S3 XPS spectra of PAS.

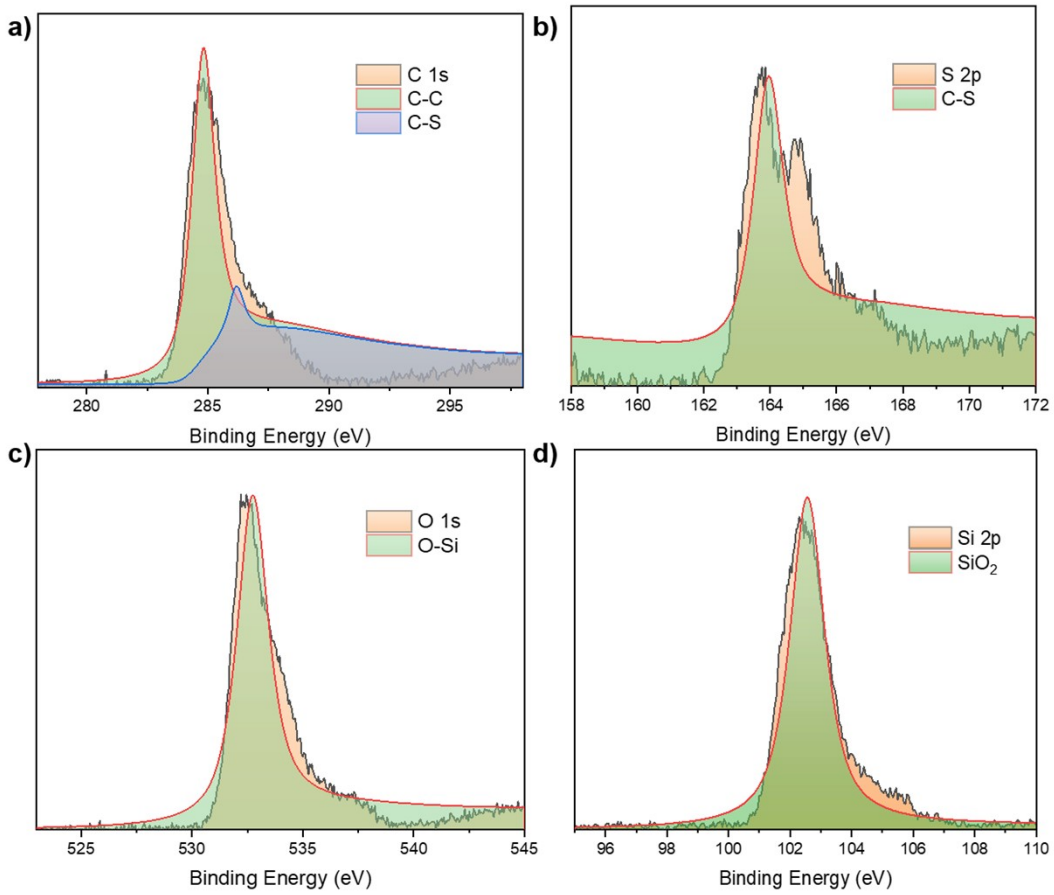

Fig. S4 XPS spectra of PSS.

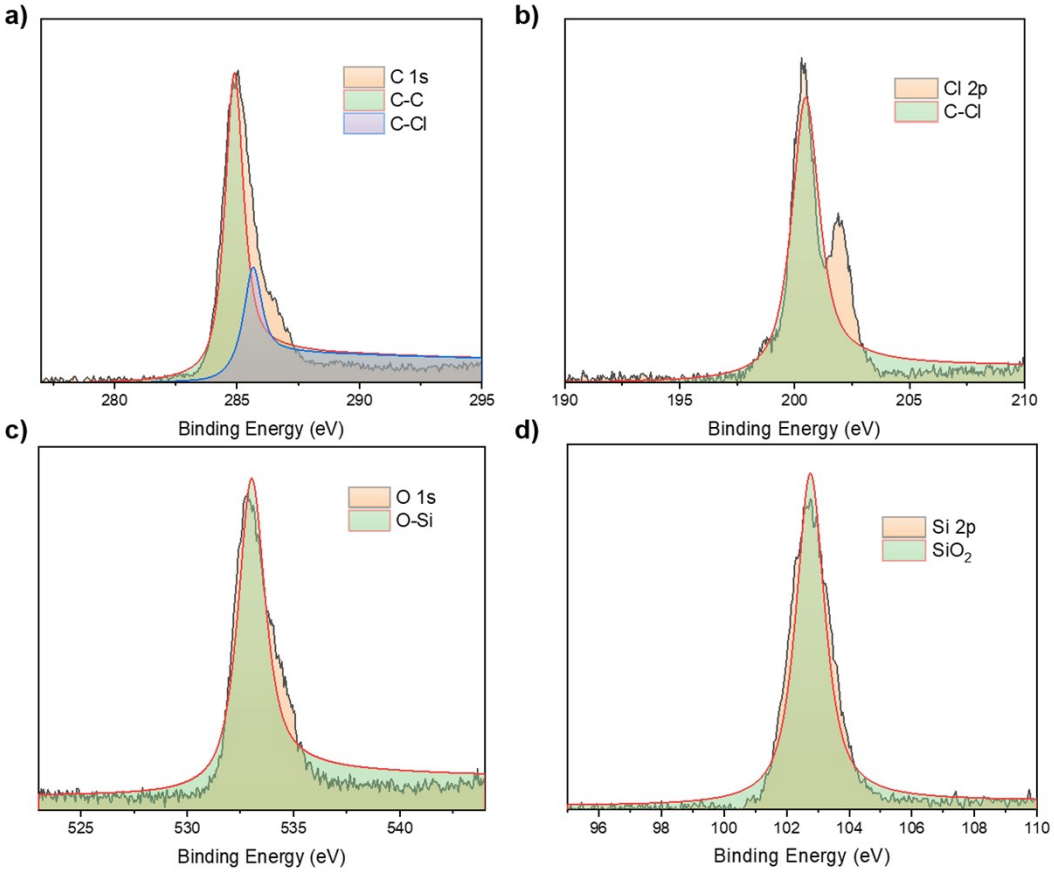

Fig. S5 XPS spectra of PCS.

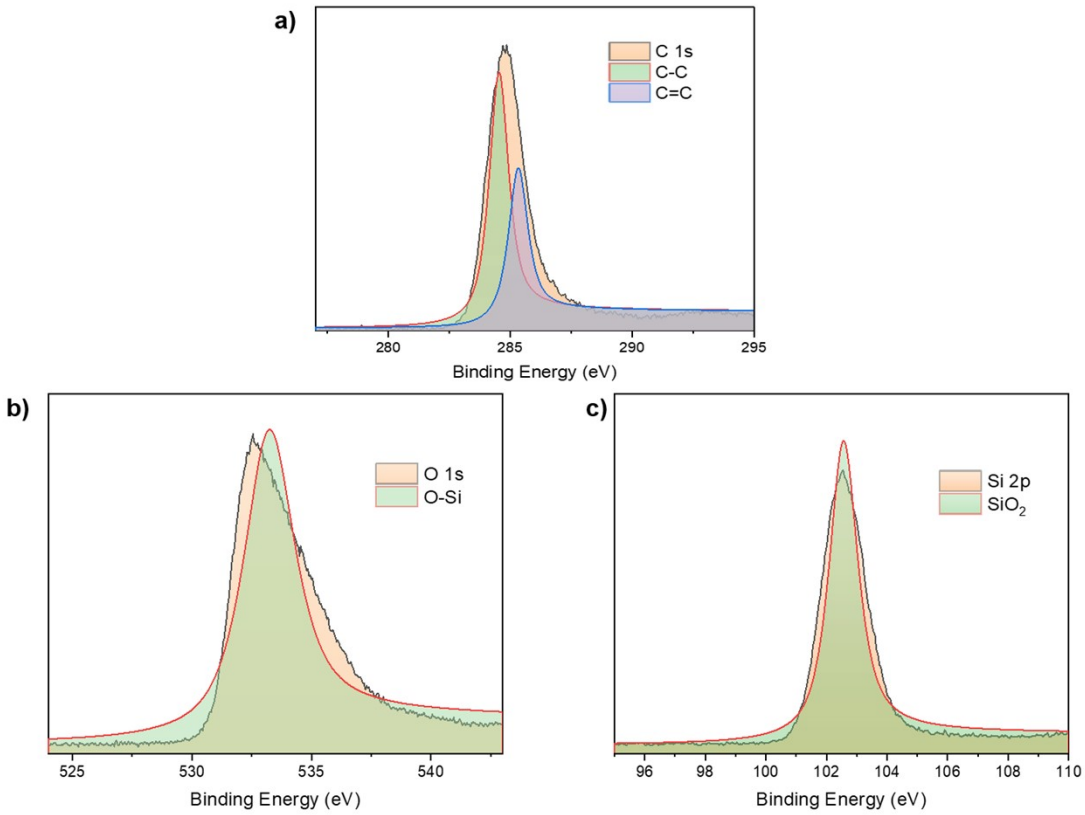

Fig. S6 XPS spectra of PVS.

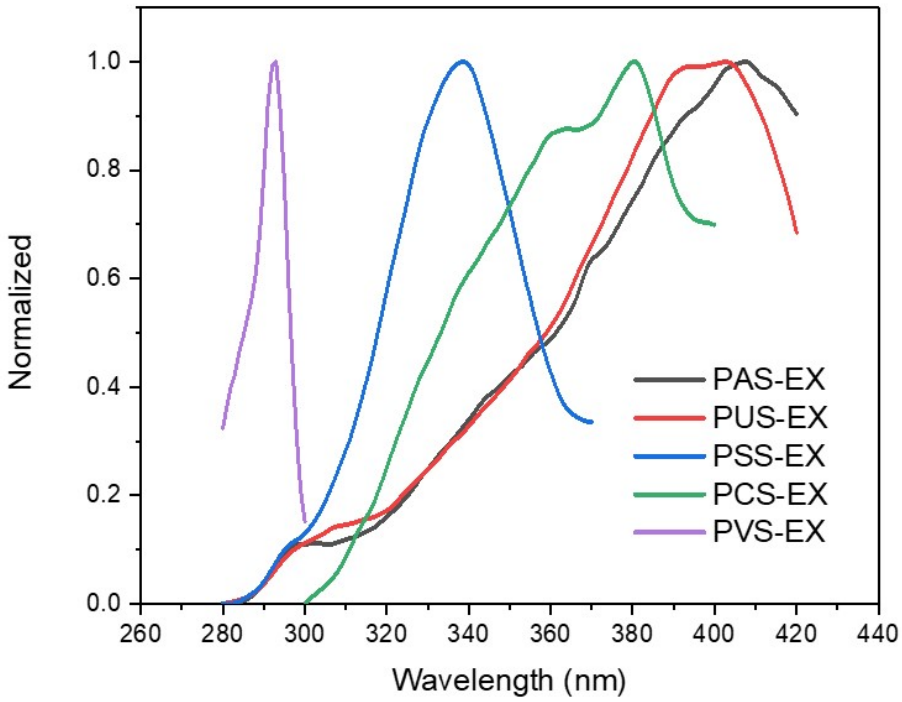

Fig. S7 Excitation spectra of PAS, PUS, PSS, PCS and PVS monitored at 452 nm, 455 nm, 378 nm, 440 nm and 357 nm, respectively.

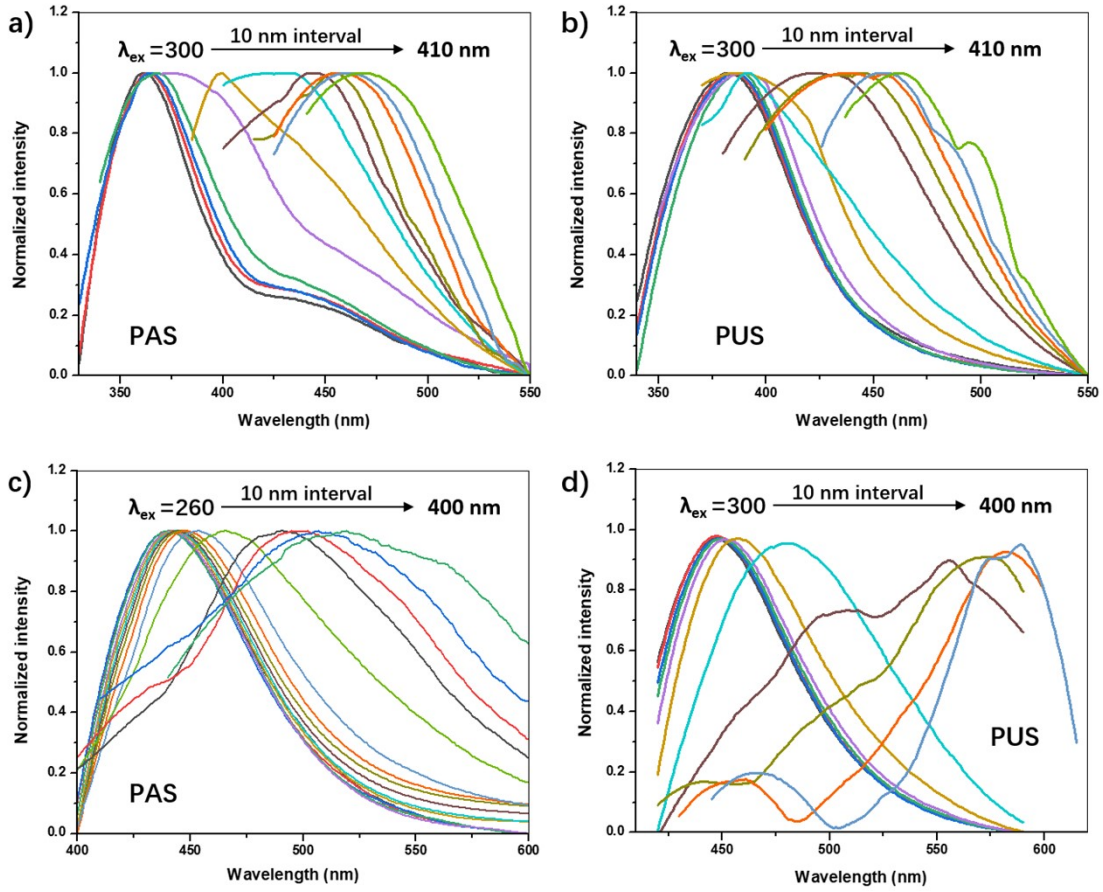

Fig. S8 Prompt (a, b) and delayed (c, d) emission spectra of PAS (a, c) and PUS (b, d) excited at different wavelength.

Table S2 Photophysical data of polysiloxane nanoparticles.

Sample	Fluorescence		Phosphorescence		Φ^a
	λ_{ex}/nm	λ_{em}/nm	λ_{em}/nm	τ/ms	
PAS	407	452	498	120.06	30.2%
PUS	403	455	485	120.40	24%
			653	91.60	
PSS	340	378	—	—	1.91%
PCS	380	440	—	—	5.66%
PVS	293	357	—	—	10.5%

[a] Total luminescence quantum yield.

Table S3 Lifetime data of PAS and PUS.

Sample	λ_{em} /nm	τ_1 /ms	τ_2 /ms	τ_3 /ms	τ_4 /ms	τ_{avg} /ms	X^2
PAS	498	13.39 (38.63%)	45.17 (37.19%)	236.66 (17.76%)	871.72 (6.43%)	120.05	1.097
PUS	485	12.23 (40.88%)	73.55 (41.94%)	491.87 (17.19%)		120.40	1.271
	653	6.71 (30.83%)	34.93 (44.96%)	305.08 (24.20%)		91.60	1.068

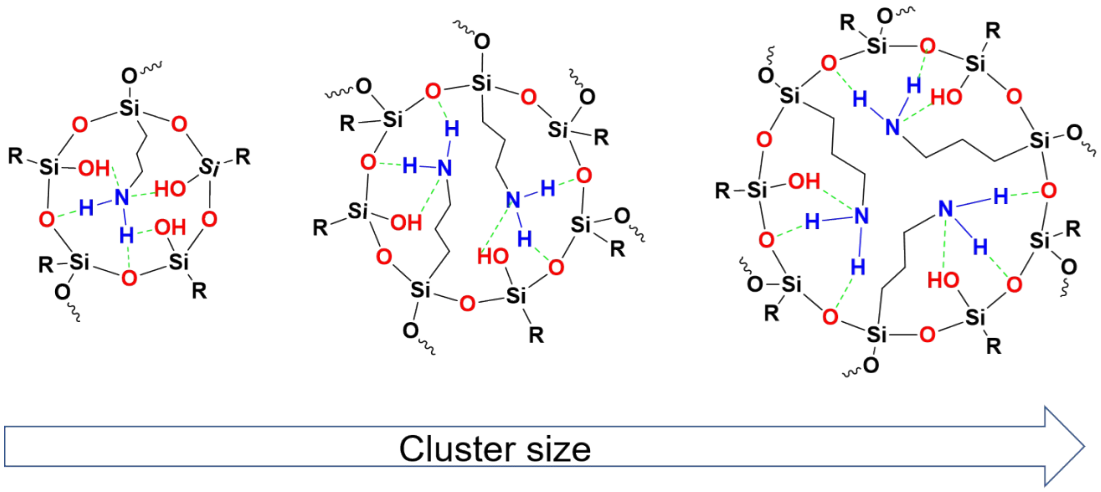

Fig. S9 Possible PAS clusters of different sizes.

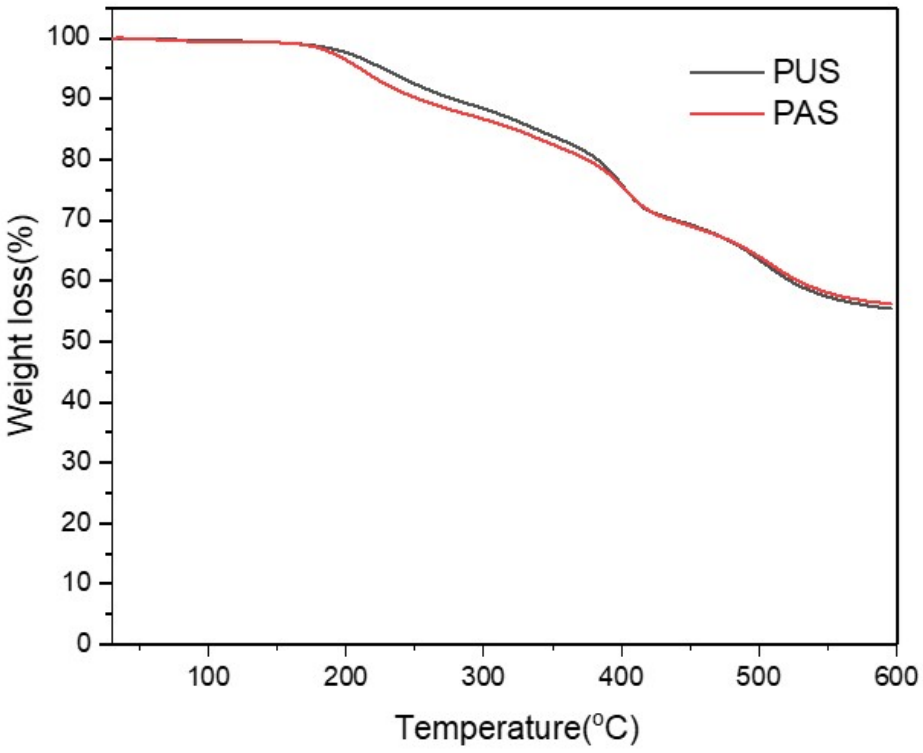

Fig. S10 Thermogravimetric analysis of PUS and PAS.

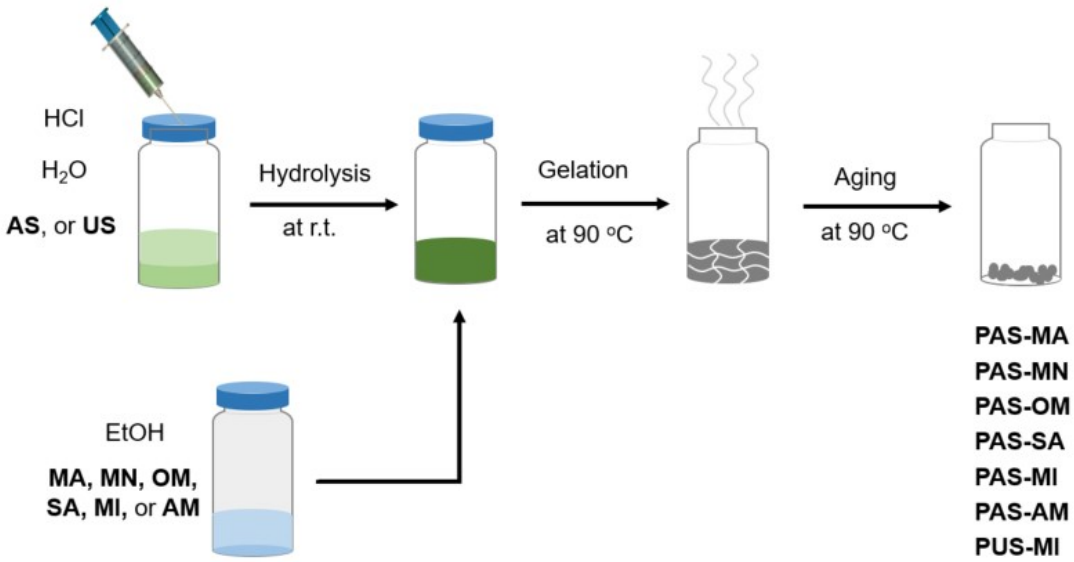

Scheme S2 Synthesis process of nanocomposites based on doped polysiloxanes.

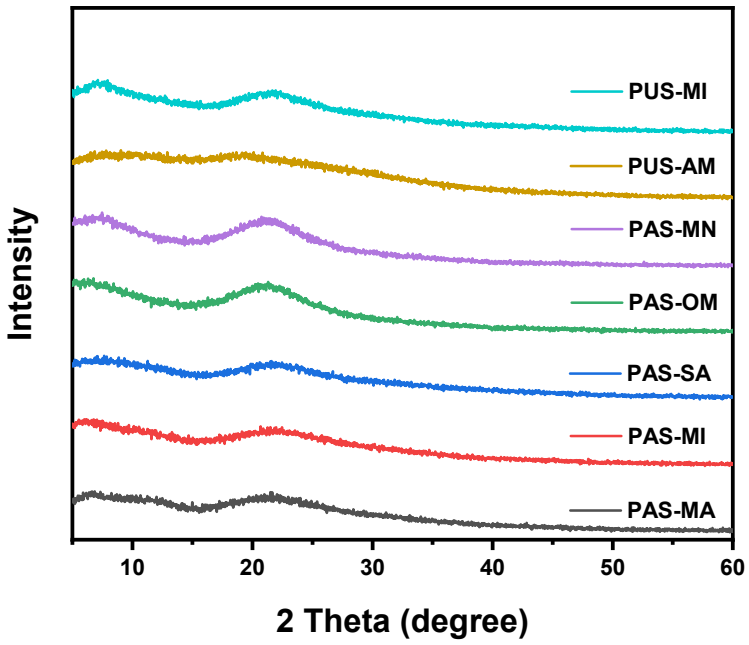

Fig. S11 PXRD curves of polysiloxane composites.

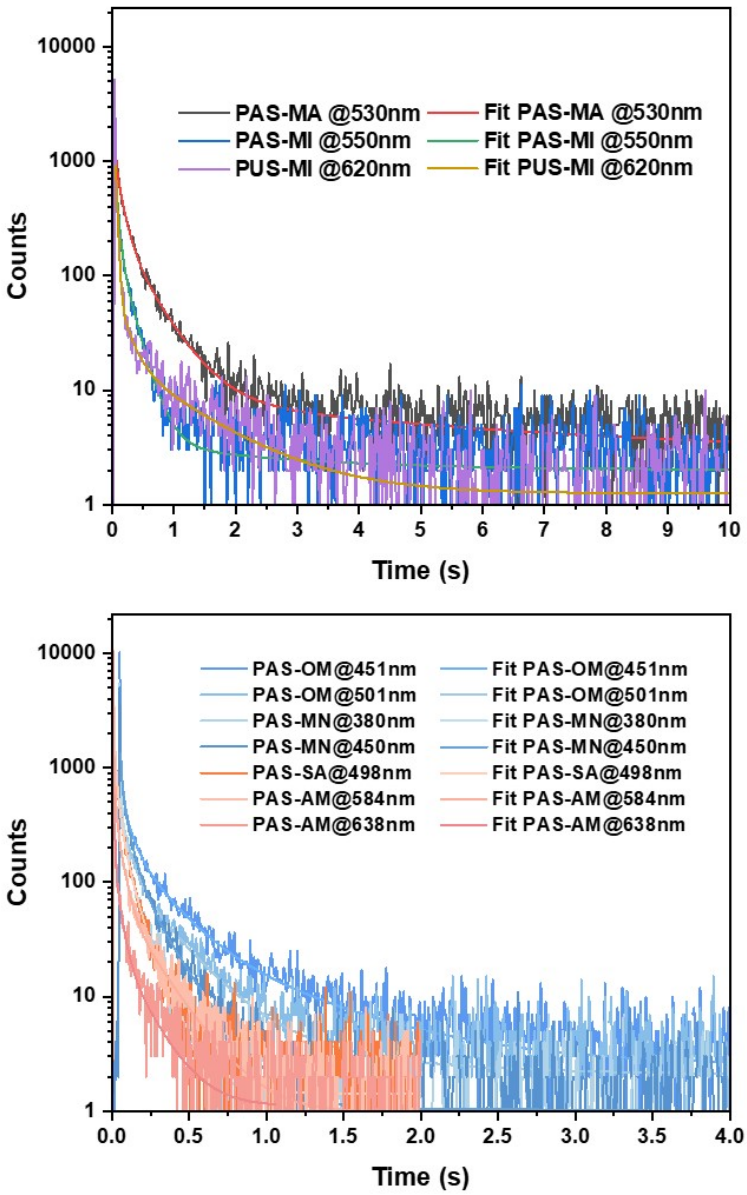

Fig. S12 Time-resolved luminescence decay profiles of polysiloxane composites.

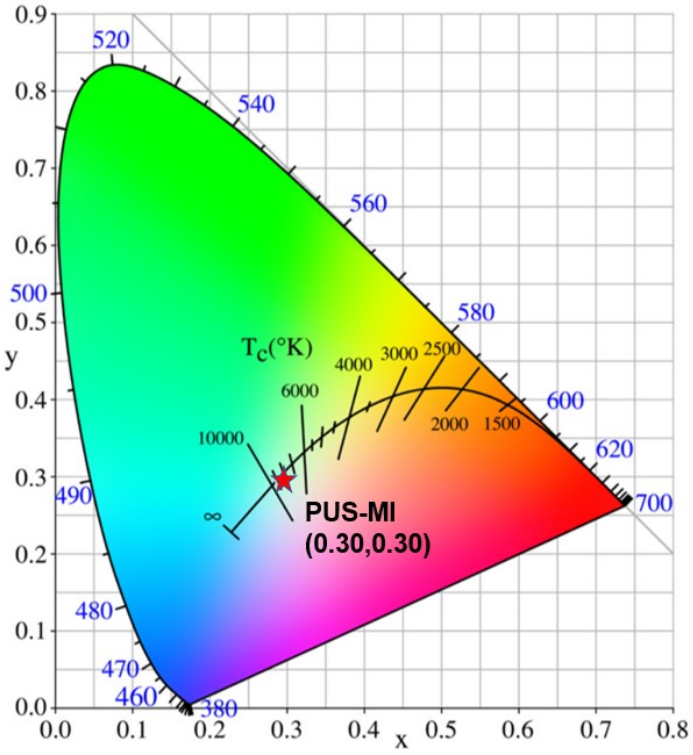

Fig. S13 Coordinate diagram of PUS-MI.

Table S4 Lifetime data of composites.

Sample	λ_{em} /nm	τ_1 /ms	τ_2 /ms	τ_3 /ms	τ_4 /ms	τ_{avg} /ms	X^2
PAS-MA	530	20.65 (23.43%)	108.68 (34.52%)	442.98 (33.64%)	4580.66 (8.40%)	576.15	1.211
PAS-MI	550	14.78 (30.15%)	54.03 (34.16%)	239.22 (29.30%)	2522.80 (6.40%)	254.46	1.183
PUS-MI	620	27.14 (60.35%)	180.56 (14.43%)	1109.99 (25.22%)		322.37	1.116
PAS-OM	451	13.90 (18.91%)	118.45 (40.45%)	522.53 (40.64%)		262.90	1.233
	501	22.96 (33.85%)	133.99 (34.41%)	626.33 (31.75%)		252.74	1.263
PAS-MN	380	4.76 (29.05%)	39.18 (35.82%)	148.44 (35.14%)		67.58	1.036
	450	7.58 (20.39%)	50.96 (39.76%)	278.18 (39.85%)		132.67	1.007
PAS-SA	498	2.84 (21.96%)	17.23 (30.08%)	63.61 (32.70%)	149.96 (15.26%)	49.49	1.195
PAS-AM	584	7.99 (22.79%)	41.73 (41.59%)	207.29 (35.61%)		92.99	1.069
	638	6.02 (18.52%)	34.69 (41.40%)	160.97 (40.08%)		79.99	1.209

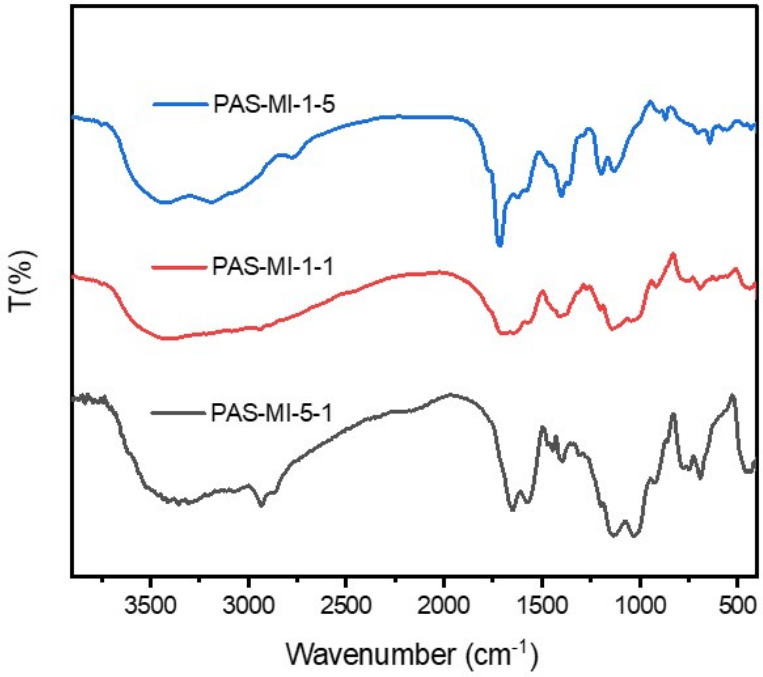

Fig. S14 FT-IR spectra of PAS-MI composites with different ratio of AS and MI (5:1, 1:1 and 1:5).

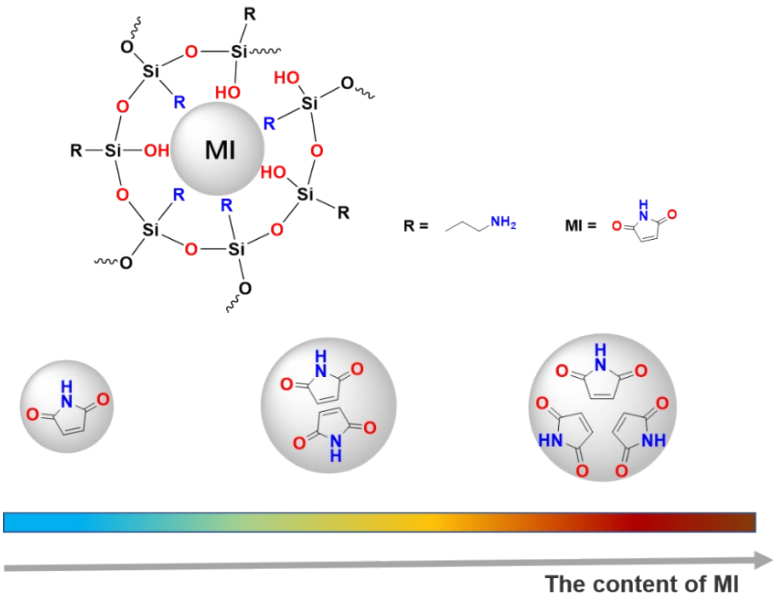

Fig. S15 Possible cluster model of PAS-MI.

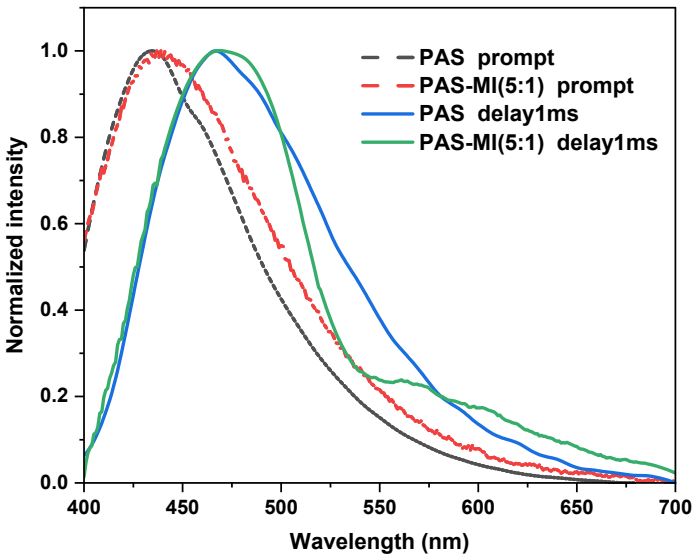

Fig. S16 Prompt (solid lines) and delayed (dotted lines) spectra of PAS and PAS-MI (5:1), excited at 354 nm.

Table S5 Photophysical properties of PAS-MI with different ratio of AS and MI.

Sample	Ratio	Fluorescence		Phosphorescence		
		λ_{ex} /nm	λ_{em} /nm	λ_{ex} /nm	λ_{em} /nm	τ /ms
PAS-MI	5:1	354	440	354	470	42
	1:1	410	507	347	550	254.46
	1:5	450	640	450	693	15.09
					753	0.163

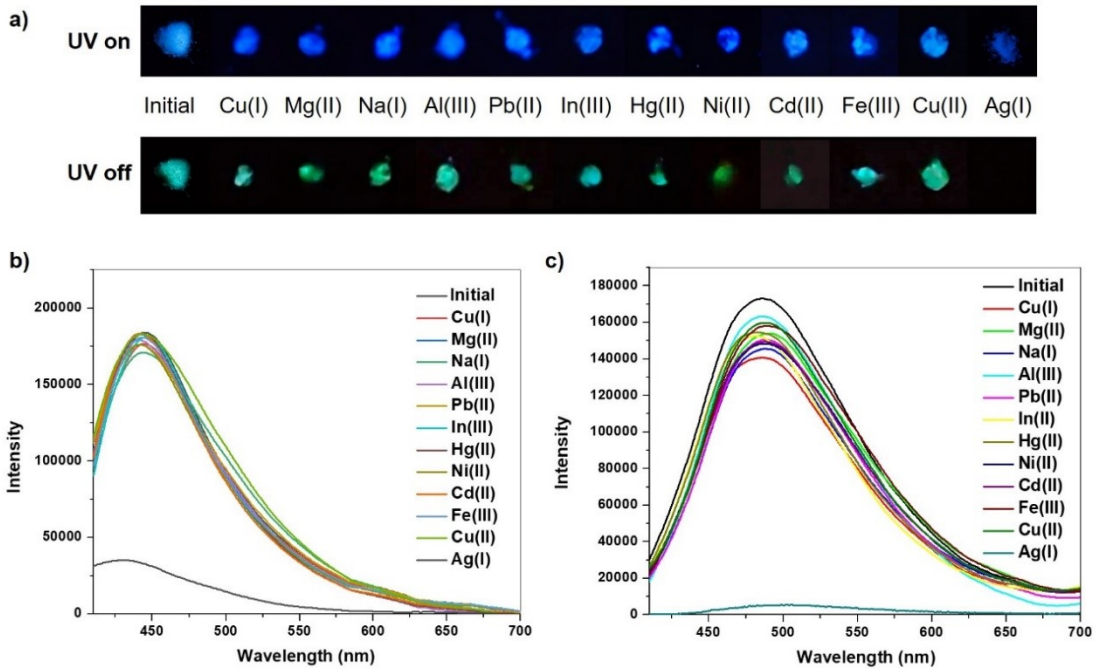

Fig. S17 a) Photographs of PAS treated by different ionic solutions before and after turning off the UV lamp. Prompt (b) and delayed (c) photoluminescence spectra of PAS after immersion in different metal ion solutions (Concentration of 2 mM, λ_{ex}=365 nm, t_d = 1ms)

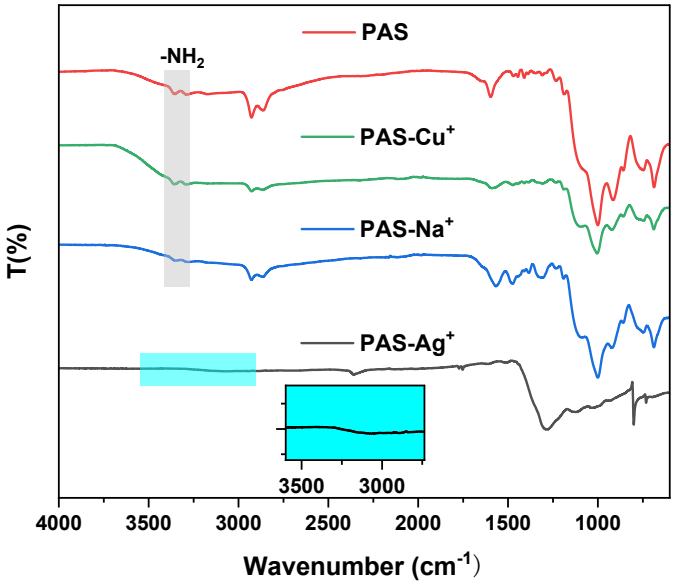

Fig. S18 In-situ ATR-IR spectra of PAS, and treated PAS by Cu^{+} (PAS-Cu^{+}), Na^{+} (PAS-Na^{+}), and Ag^{+} (PAS-Ag^{+}). Inset: local enlarged drawing of PAS-Ag^{+}.

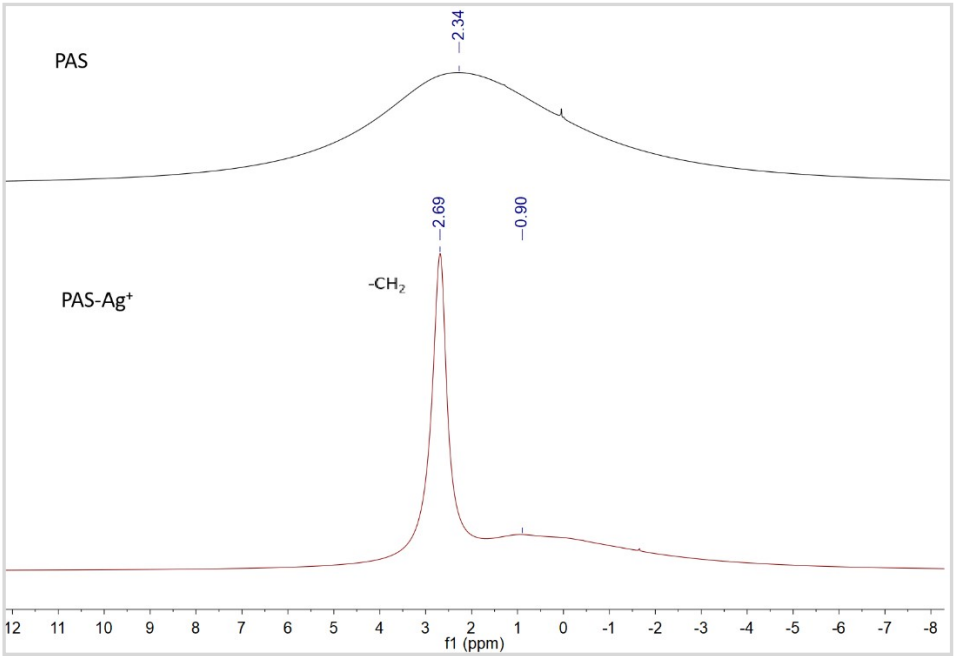

Fig. S19 Solid-state NMR of PAS and treated PAS by Ag^{+} (PAS-Ag^{+}).

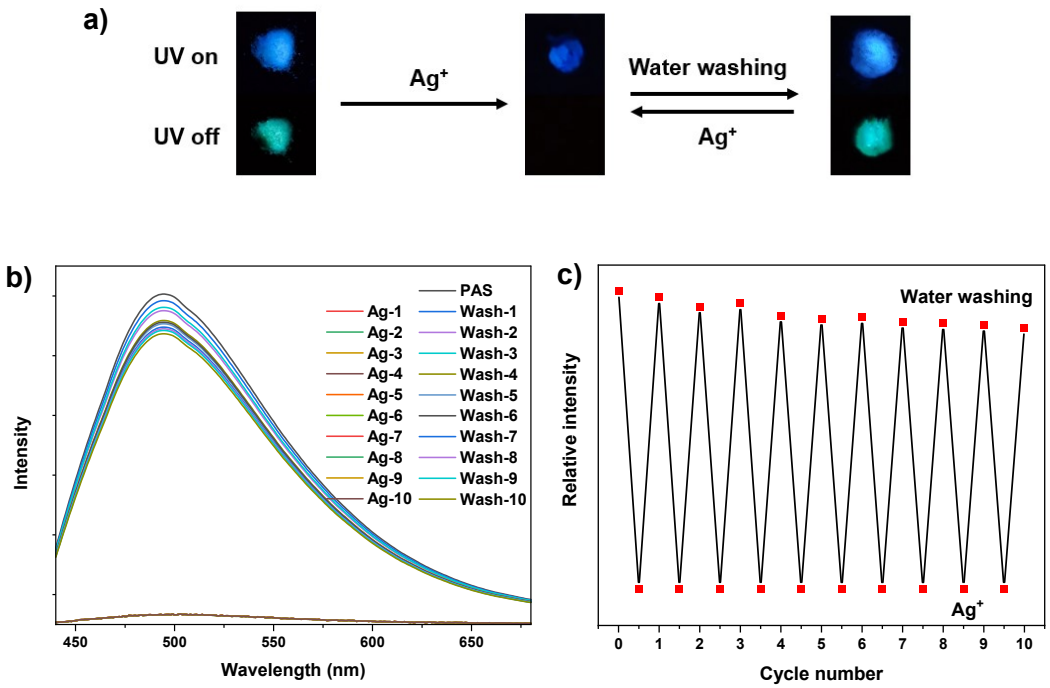

Fig. S20 a) Switching of PAS luminescence; b) delayed photoluminescence spectra of the PAS (t_d = 1ms); c) PAS light-emitting switching cycle.

Table S6 Charge/radius ratio (z/r) of the metal ions used in this paper.[13]

Ions	z/r	Ions	z/r
Cu^{+}	1.04	In^{3+}	3.7
Cu^{2+}	2.78	Pb^{2+}	1.96
Mg^{2+}	3.03	Hg^{2+}	1.82
Na^{+}	1.03	Ni^{2+}	2.89
Al^{3+}	5.88	Cd^{2+}	2.06
Fe^{3+}	4.69	Ag^{+}	0.79

Reference

1 S. Yu, Z. Wang, L. Gao, B. Zhang, L. Wang, J. Kong and L. Li, A Highly Selective and Sensitive Peptide-Based Fluorescent Ratio Sensor for Ag^{+}, *J Fluoresc.*, 2021, **31**, 237-246.

2 Y. Wei, B. Li, X. Wang and Y. Duan, Magnified fluorescence detection of silver(I) ion in aqueous solutions by using nano-graphite-DNA hybrid and DNase I, *Biosens. Bioelectron.*, 2014, **58**, 276-281.

3 Y. Wang, X. Bin, X. Chen, S. Zheng, Y. Zhang and W. Z. Yuan, Emission and Emissive Mechanism of Nonaromatic Oxygen Clusters, *Macromol. Rapid Commun.*, 2018, **39**, e1800528.

4 A. Safavi, R. Ahmadi and Z. Mohammadpour, Colorimetric sensing of silver ion based on anti aggregation of gold nanoparticles, *Sens. Actuators, B*, 2017, **242**, 609-615.

5 J. H. Kim, K. B. Kim, J. S. Park and N. Min, Single cytosine-based electrochemical biosensor for low-cost detection of silver ions, *Sens. Actuators, B*, 2017, **245**, 741-746.

6 X.-E. Zhao, C. Lei, Y. Gao, H. Gao, S. Zhu, X. Yang, J. You and H. Wang, A ratiometric fluorescent nanosensor for the detection of silver ions using graphene quantum dots, *Sens. Actuators, B*, 2017, **253**, 239-246.

7 L. He, Y. Lu, F. Wang, W. Jing, Y. Chen and Y. Liu, Colorimetric sensing of silver ions based on glutathione-mediated MnO2 nanosheets, *Sens. Actuators, B*, 2018, **254**, 468-474.

8 J. Wang, Z. Lan, S. Hou and S. Hou, A novel symmetrical imidazole-containing framework as a fluorescence sensor for selectively detecting silver ions, *Analyst*, 2021, **146**, 7618-7626.

9 Z.-F. Pu, J. Peng, Q.-L. Wen, Y. Li, J. Ling, P. Liu and Q.-E. Cao, Photocatalytic synthesis of BSA-Au nanoclusters with tunable fluorescence for highly selective detection of silver ion, *Dyes Pigm.*, 2021, **193**, 109533.

10 C. Zhao, X. Kong, S. Shuang, Y. Wang and C. Dong, An anthraquinone-imidazole-based colorimetric and fluorescent sensor for the sequential detection of Ag(+) and biothiols in living cells, *Analyst*, 2020, **145**, 3029-3037.

11 Q. Lai, Q. Liu, Y. He, K. Zhao, C. Wei, L. Wojtas, X. Shi and Z. Song, Triazole-imidazole (TA-IM) derivatives as ultrafast fluorescent probes for selective

Ag(+) detection, *Org. Biomol. Chem.*, 2018, **16**, 7801-7805.

12 J. Wang, A. Y. Liu, B. C. Wu, Q. L. Wen, Z. F. Pu, R. X. Zhao, J. Ling and Q. Cao, Highly selective and rapid detection of silver ions by using a "turn on" non-fluorescent cysteine stabilized gold nanocluster probe, *Anal. Methods*, 2021, **13**, 2099-2106.

13 H. Grünewald, Handbook of Chemistry and Physics. By R. C. Weast, *Angew. Chem. Int. Ed.*, 1972, **11**, 449-449.